sustainability

MDPI

Article

Slow Pyrolysis of *Ulva lactuca* (Chlorophyta) for Sustainable Production of Bio-Oil and Biochar

Apip Amrullah [1], Obie Farobie [2,3], Asep Bayu [4], Novi Syaftika [5], Edy Hartulistiyoso [2,3], Navid R. Moheimani [6], Surachai Karnjanakom [7] and Yukihiko Matsumura [8]

1 Department of Mechanical Engineering, Lambung Mangkurat University, Banjarmasin 70123, Indonesia; apip.amrullah@ulm.ac.id
2 Department of Mechanical and Biosystem Engineering, Faculty of Agricultural Engineering and Technology, IPB University (Bogor Agricultural University), IPB Darmaga Campus, P.O. Box 220, Bogor 16002, Indonesia; edyhartulistiyoso@apps.ipb.ac.id
3 Surfactant and Bioenergy Research Center (SBRC), IPB University (Bogor Agricultural University), Bogor 16144, Indonesia
4 Research Center for Biotechnology, Research Organization for Life Sciences, National Research and Innovation Agency (BRIN), Jl. Raya Jakarta-Bogor KM 46 Cibinong, Bogor 16911, Indonesia
5 Center for Energy Resource and Chemical Industry Technology, Research Organization for Assessment and Application of Technology, National Research and Innovation Agency (BRIN), Jakarta Pusat 10340, Indonesia; novi017@brin.go.id
6 Algae R&D Centre, Harry Butler Institute, Murdoch University, Murdoch, WA 6150, Australia; n.moheimani@murdoch.edu.au
7 Department of Chemistry, Faculty of Science, Rangsit University, Pathumthani 12000, Thailand; surachai.ka@rsu.ac.th
8 Graduate School of Advanced Science and Engineering, Hiroshima University, Higashi-Hiroshima 739-8527, Japan

check for updates

Citation: Amrullah, A.; Farobie, O.; Bayu, A.; Syaftika, N.; Hartulistiyoso, E.; Moheimani, N.R.; Karnjanakom, S.; Matsumura, Y. Slow Pyrolysis of *Ulva lactuca* (Chlorophyta) for Sustainable Production of Bio-Oil and Biochar. *Sustainability* **2022**, *14*, 3233. https://doi.org/10.3390/su14063233

Academic Editors: Baojie He, Ayyoob Sharifi, Chi Feng and Jun Yang

Received: 2 February 2022
Accepted: 7 March 2022
Published: 9 March 2022

Publisher's Note: MDPI stays neutral with regard to jurisdictional claims in published maps and institutional affiliations.

Abstract: *Ulva Lactuca* is a fast-growing algae that can be utilized as a bioenergy source. However, the direct utilization of *U. lactuca* for energy applications still remains challenging due to its high moisture and inorganics content. Therefore, thermochemical processing such as slow pyrolysis to produce valuable added products, namely bio-oil and biochar, is needed. This study aims to conduct a thorough investigation of bio-oil and biochar production from *U. lactuca* to provide valuable data for its further valorization. A slow pyrolysis of *U. lactuca* was conducted in a batch-type reactor at a temperature range of 400–600 °C and times of 10–50 min. The results showed that significant compounds obtained in *U. lactuca*'s bio-oil are carboxylic acids (22.63–35.28%), phenolics (9.73–31.89%), amines/amides (15.33–23.31%), and N-aromatic compounds (14.04–15.68%). The ultimate analysis revealed that biochar's H/C and O/C atomic ratios were lower than feedstock, confirming that dehydration and decarboxylation reactions occurred throughout the pyrolysis. Additionally, biochar exhibited calorific values in the range of 19.94–21.61 MJ kg^{-1}, which is potential to be used as a solid renewable fuel. The surface morphological analysis by scanning electron microscope (SEM) showed a larger surface area in *U. lactuca*'s biochar than in the algal feedstock. Overall, this finding provides insight on the valorization of *U. lactuca* for value-added chemicals, i.e., biofuels and biochar, which can be further utilized for other applications.

Keywords: thermochemical conversion; biomass; seaweed; biofuel; algae

1. Introduction

Biomass-derived bioenergy has received much interest as a renewable energy option to replace fossil fuels, owing to its potential to provide sustainable energy, abundance, carbon-neutrality, low cost, and inherently environmental friendliness [1,2]. Several methods are developed to produce energy from biomass, including biological and thermochemical processes. Biological conversion is considered a less energy-intensive process than the

thermochemical route, but it has shortcomings due to long processing times and rigorous requirements of temperature and pH [3]. Thermochemical processes of gasification, torrefaction, and pyrolysis are considered favorable due to them being more cost-effective and efficient [4–6]. Pyrolysis is a thermochemical process that has received much interest in recent years as a cost-effective and energy-efficient process for biomass conversion to biofuels and valuable chemicals [7]. Principally, pyrolysis is conducted by biomass conversion at a temperature between 300 and 600 °C in the absence of oxygen, generating three main products, i.e., bio-oil, biochar, and syngas [8]. Pyrolysis has recently been recognized as a viable approach for managing some biomass sources for the simultaneous production of high-calorific-value liquid and gas products, as well as a carbon-rich solid that can be utilized as activated carbon, soil ameliorant, etc. [9].

In the context of utilization and source, biomass is classified into first-, second-, third-, and fourth generations. The exploitation of first- and second-generation biomass not only triggers the food versus fuel debate, but also increases the inflation of food prices, and requiring fresh water and arable land [10]. To ensure the sustainability of biomass-derived energy, the diversification of biomass sources is vital, especially concerning the use of freshwater and arable land to supply biomass. It is needless to say that fresh water demand keeps increasing due to the rapid growth in world population leading to the limitation of freshwater for biomass cultivation [10]. Therefore, as the third generation of biomass, marine macroalgae (seaweeds) are expected to play a vital role as a source of biomass since they have a rapid growth rate and high-value compounds, including polysaccharides, protein, and bioactive molecules [11,12]. Further, marine macroalgae do not compete with food crops over fresh water and arable land [13,14].

Ulva is considered to be one of the most promising macroalgal biomass sources, since it is a fast-growing green macroalga that may be found abundantly all over the world [15,16]. Indeed, species identified in genus *Ulva* are well known for their ability to uptake organic materials and ease of cultivation [17]. They can absorb heavy metals and organic pollutants [18]. Additionally, *Ulva* is gaining more interest since their growth rates can be five times faster than corn, making them a potential contender as a source of bioenergy feedstock [19]. Having said that, *Ulva* has also been reported as the most common algae, besides water hyacinth and Sargassum, which can cause severe aquatic problems due to excessive growth and eutrophication [20–24]. In this sense, the valorization of *Ulva* would be beneficial not only for meeting the requirement of renewable energy sources but also for environmental mitigation. Additionally, the utilization of macroalgae as a viable source of renewable energy would give a promising option to energy security and tackle global concerns due to fossil fuel scarcity and global warming. However, the direct utilization of *U. lactuca* for energy applications still remains challenging due to its high moisture and inorganics content, but low calorific value. Therefore, thermochemical processing such as slow pyrolysis to produce value-added products, namely bio-oil and biochar, is required.

A number of studies concerning bio-oil and biochar production from algae have reported that sustainable solid and liquid biofuels can be generated from macroalgae via pyrolysis [8,25–31]. Nevertheless, very little information is available on bio-oil and biochar production from *Ulva* [32–34]. It should be noted that most of the previous studies only focused on the characteristics of bio-oil. A comprehensive study not only focusing on bio-oil but also biochar is necessary, since biochar has excellent potential as a carbon material for catalyst, pollutant removal, energy storage, and CO_2 capture [35]. Meanwhile, after being upgraded, bio-oil can be used as a substitute for fossil resources for various applications, such as fuel to generate heat and power and for chemical production. Apart from that, the most used green algae for bio-oil and biochar production in previous works is *U. prolifera*. The valorization of *U. lactuca* for bio-oil and biochar production via pyrolysis has not been studied well. Therefore, this study aims to investigate the bio-oil and biochar production as well as their characteristics from *U. lactuca* via slow-pyrolysis.

The new finding of this study is highlighted as follows: (1) performing a comprehensive study for the coproduction of bio-oil and biochar from *U. lactuca*, including their characteristics which have not been reported elsewhere and (2) providing the detailed reaction pathway for the conversion of *U. lactuca* into high-value compounds identified in bio-oil.

2. Materials and Methods

2.1. Feedstock Preparation

A green macroalgal feedstock, *U. lactuca*, was obtained at Ekas beach, Pemongkong, East Lombok Regency, West Nusa Tenggara, Indonesia. To remove sand and debris, the fresh macroalgal feedstock was washed with tap water followed by distilled water. Subsequently, the macroalgal sample was dried in an oven for 3 h at 50 °C. Afterwards, the sample was ground in a coffee bean grinder and sieved to create a consistent particle size of 0.25 mm.

2.2. Feedstock Characterization

The proximate analysis of feedstock was conducted using a thermogravimetric analyzer TGA 4000 (Perkin Elmer, United States) following ASTM E1131-08. The feedstock's moisture content (MC) was calculated after the sample was heated to 110 °C under inert conditions using pure N_2. Meanwhile, the volatile matter (VM) was determined from the mass loss after heating the sample to 900 °C. The ash content (AC) was calculated as the amount of sample that remained after 45 min of isothermal heating at 900 °C by switching the N_2 to air. The fixed carbon (FC) value was calculated using the formula as depicted in Equation (1) below:

$$\text{FC (wt\%)} = 100 - [\text{VM (wt\%)} + \text{MC (wt\%)} + \text{AC (wt\%)}] \quad (1)$$

Higher heating values (HHVs) of *U. lactuca* were calculated using a bomb calorimeter (Parr 6200 Isoperibol) in accordance with ASTM D 5865-04. A CHN628 analyzer (Leco) was used to determine the final contents of carbon (C), hydrogen (H), and nitrogen (N). Meanwhile, a CHN632 analyzer (Leco) was employed to measure the sulfur (S) content. The content of oxygen (O) was determined using the formula as follow:

$$\text{O (\%)} = 100 - (\%\text{C} + \%\text{H} + \%\text{N} + \%\text{S}) \quad (2)$$

Each analysis was conducted three times until the reproducible data were achieved. Table S1 presents the proximate and ultimate analyses of *U. lactuca*.

2.3. Pyrolysis of U. lactuca

The feedstock was pyrolyzed in a stainless batch-type reactor as schematically illustrated in Figure 1. The reactor was equipped with a thermocouple, an electric furnace, and a condenser. The maximum operating temperature of the reactor is 1000 °C, which is controlled using a PID temperature controller. A 50 g dried *U. lactuca* was placed inside the reactor. To ensure an oxygen-free atmosphere, the reactor was purged with N_2 prior to the pyrolysis process at a flow rate of 100 mL min^{-1}. Please note that all experiments were conducted at atmospheric pressure. The reactor was heated at a rate of 30 °C min^{-1} from ambient to the final temperatures of 400, 500, and 600 °C.

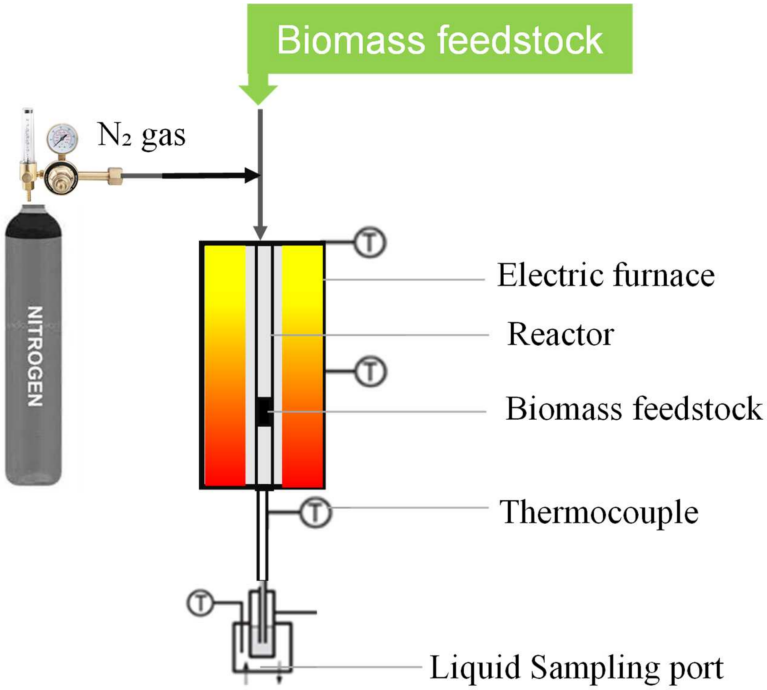

Figure 1. The pyrolysis reactor of *U. lactuca*.

Vapor-phase products were condensed and collected in a liquid sample port during pyrolysis. The biochar was collected after cooling down the reactor, and the mass was weighed using gravimetry. All of the experiments were carried out twice. The yield of the products is calculated using the equations listed below.

$$\text{Bio-oil yield } (\%) = \frac{W_{bio-oil}}{W_{initial\ feedstock\ (dry)}} \times 100 \quad (3)$$

$$\text{Solid yield } (\%) = \frac{W_{solid\ product}}{W_{intial\ feedstock\ (dry)}} \times 100 \quad (4)$$

$$\text{Gas yield } (\%) = 100 - (bio - oil + solid\ product) \quad (5)$$

2.4. Product Characterization

The bio-oil was characterized using a gas chromatography-mass spectrometry (GC/MS-QP2010 SE–Shimadzu, Japan) system with an Rtx®-5MS capillary column. The details of bio-oil analysis have been reported in our previous studies [36,37]. In brief, the temperature of GC was initially set at 150 °C for 5 min. The temperature was then ramped to 300 °C at a rate of 10 °C min^{-1}. The oven was maintained at this temperature for 26 min. The NIST2008 c2.0/Xcalibur data library was used to compare recorded mass spectra to determine the bio-oil compounds.

The biochar was analyzed using an elemental (C, H, N, S) analyzer, scanning electron microscopy (SEM), and a Fourier transform infrared spectroscopy (FTIR). The elemental composition of solid products (C, H, N, S, O) was determined using the same procedures as feedstock. A scanning electron microscopy (SEM) (Hitachi, SU 3500) was used to observe the morphology of the solid product with the magnifications of 1000 and 2500×. To evaluate the appearance of functional groups in the biochar, FTIR analysis was conducted using infrared spectrometer Spectrum Two Universal ATR–FT-IR (Perkin Elmer, Waltham, MA, USA).

3. Results and Discussion

3.1. Product Yield Distribution at the Different Reaction Temperature

The effect of temperature on product yield distribution from the pyrolysis of *U. lactuca* at the temperature range of 400–600 °C is summarized in Figure 2. At 400 °C, bio-oil yields were still relatively low. Bio-oil yields of merely 7.82, 12.49, and 14.32% were obtained for reaction times of 10, 30, and 50 min, respectively, reflecting incomplete pyrolysis of *U. lactuca* at 400 °C. The bio-oil yields significantly increased with an increase in temperature of 400 to 500 °C, achieving 7.98, 17.06, and 24.05% within 10, 30, and 50 min, respectively. This trend could be attributed to; (1) more significant primary decomposition of macroalgal biomass at higher temperature and (2) secondary decomposition of biochar. As the pyrolysis temperature rose to 600 °C, the bio-oil yields slightly increased, but the prolonged reaction time did not lead to a considerable increase in bio-oil. This could be attributed to the more significant decomposition of low molecular weight compounds in the liquid phase into noncondensable gas occurring at higher temperatures and longer reaction times [38]. The bio-oil yield obtained from this study is comparable with the previous work using hydrothermal liquefaction. Yan et al. [39] reported that the highest bio-oil yield of 12.0 wt% was achieved for noncatalytic liquefaction of *Ulva prolifera* at 290 °C within 10 min. Meanwhile, the bio-oil yield increased as the KOH (0.1 g) catalyst was added, achieving the highest yield of 26.7 wt%.

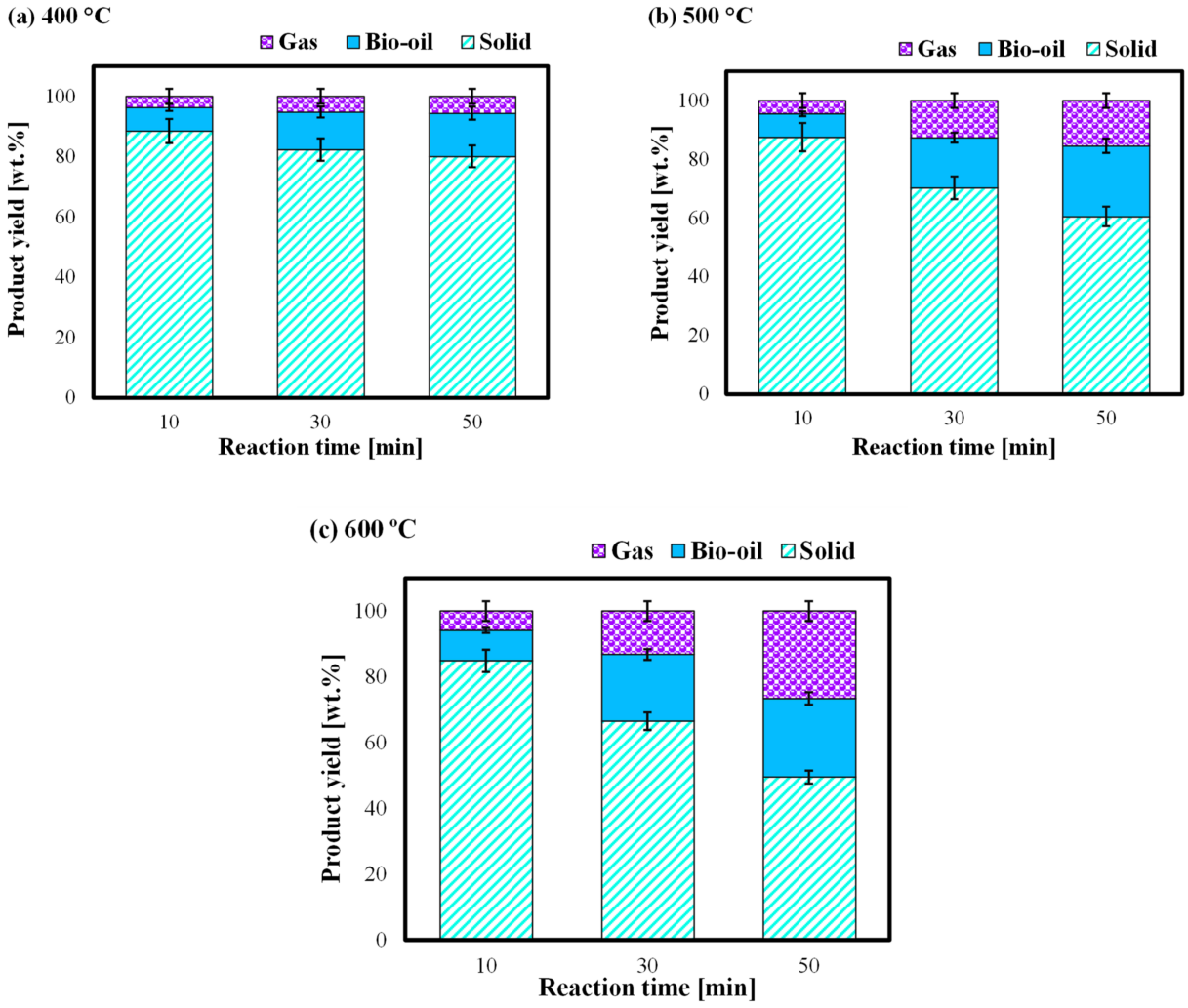

Figure 2. Product yield distribution of *U. lactuca* at the different reaction temperatures of (**a**) 400 °C, (**b**) 500 °C, and (**c**) 600 °C.

In contrast with the bio-oil yield, the biochar yield decreased with higher temperatures and longer reaction times. At 400 °C, the biochar yields decreased from 88.47 to 80.07% as the reaction time was prolonged from 10 to 50 min. A substantial decomposition of biochar was observed at higher temperatures of 500 °C, resulting in yields of 87.52, 70.29, and 60.53% at 10, 30, and 50 min, respectively. The biochar yield sharply decreased when the temperature increased to 600 °C, leading to yields of 84.85, 66.49, and 49.53% at 10, 30, and 50 min, respectively. This result could be attributed to the more considerable decomposition of macroalgal feedstock at high temperatures, resulting in a decreasing in biochar formation [31]. This finding is in accordance with previous works that reported that biochar yield significantly decreased with temperature and time [33,40].

It can be noted from this study that the gas yield remarkably increased with temperature and time. However, the effect of temperature is more significant than the reaction time. This can be explained due to the pyrolysis vapors at higher temperatures as well as the secondary cracking of the char to generate noncondensable gases, such as CH_4, CO, and CO_2, as reported by a previous study [31].

3.2. Bio-Oil Characteristics

The composition of bio-oil from the pyrolysis of *U. lactuca* was determined by GC/MS analysis. GC/MS chromatogram of bio-oil from pyrolysis of *U. lactuca* is presented in Figure S1. The bio-oil product from the *U. lactuca* pyrolysis displayed various chemicals. Table 1 summarizes the compounds identified in *U. lactuca* bio-oil at different temperatures. As shown in Table 1, the three abundant compounds obtained from the pyrolysis of *U. lactuca* are phenol, acetic acid, and 3-hydroxypyridine. The formation of phenol might be derived from the interaction of the aromatic compound with steam during the pyrolysis of biomass [41]. Meanwhile, acetic acid is derived from the thermal decomposition of lipid [10]. Apart from that, the 3-hydroxypyridine has been linked to the degradation of protein into amino acids at high pyrolysis temperature, followed by the cyclization reaction of amino acids [42].

Table 1. Compounds identified in *U. lactuca*'s bio-oil at different experimental temperatures by GC/MS.

No.	Compounds	Molecular Formula	Relative Area (%) under Different Pyrolysis Temperature		
			400 °C	500 °C	600 °C
1	Acetic acid	$C_2H_4O_2$	18.011	22.582	32.908
2	Propionic acid	$C_3H_6O_2$	1.986	2.495	1.689
3	Cyclopropane	C_3H_6	5.515	3.859	8.268
4	Acetamide	C_2H_5NO	5.030	8.535	5.061
5	Butanoic acid	$C_4H_8O_2$	1.168	1.248	0.283
6	2-Methylpyrazine	$C_5H_6N_2$	1.370	1.918	2.243
7	Isovaleric acid	$C_5H_{10}O_2$	1.463	1.693	0.404
8	2-Furanmethanol	$C_5H_6O_2$	0.462	0.263	0.283
9	3-Methylpyridine	C_6H_7N	0.631	0.294	0.283
10	2-Hexen-1-ol	$C_6H_{12}O$	2.144	0.314	0.566
11	2-Acetylfuran	C_2H_2O	2.173	1.918	1.368
12	5-Methylfurfural	$C_6H_6O_2$	1.195	1.329	2.447
13	3-Methyl-2-cyclopenten-1-one	C_6H_8O	1.370	1.745	0.423
14	Phenol	C_6H_6O	27.671	18.130	8.106
15	2,3-Dimethyl-2-cyclopente-1-one	$C_7H_{10}O$	0.713	0.593	1.324
16	*o*-Cresol	C_7H_8O	0.920	0.697	0.283
17	*p*-Cresol	C_7H_8O	3.295	1.337	1.346
18	3-Hydroxypyridine	C_5H_5NO	9.864	8.483	9.015
19	2-(2-Butoxyethoxy) ethanol	$C_8H_{18}O_3$	0.727	0.213	0.280
20	Ethyl methacrylate	$C_6H_{10}O_2$	0.660	1.195	1.681
21	2-Hyrodxy-5-methylacetophenone	$C_9H_{10}O_2$	0.555	1.428	5.000

Table 1. *Cont.*

No.	Compounds	Molecular Formula	Relative Area (%) under Different Pyrolysis Temperature		
			400 °C	500 °C	600 °C
22	5-Methylhydantoin	$C_4H_6N_2O_2$	2.781	4.981	2.499
23	4-(2-Aminoethyl) morpholine	$C_6H_{14}N_2O$	1.458	1.445	1.763
24	4-Octadecylmorpholine	$C_{22}H_{45}NO$	5.787	6.718	10.429
25	Propanamide	C_3H_7NO	0.622	1.767	0.799
26	Hexanamide	$C_6H_{13}NO$	0.917	1.871	0.722
27	2-Pyrrolidinone	C_4H_7NO	1.206	1.964	0.291
28	4-methylpentanamide	$C_6H_{13}NO$	0.310	1.009	0.253

Compounds obtained from the pyrolysis of *U. lactuca* as shown in Table 1 can be classified into several groups, namely aliphatic hydrocarbon, amines/amides, carboxylic acids, furan derivatives, ketones, N-aromatic compounds, and phenolic compounds (Figure 3). Carboxylic acid was the most predominant compound observed from the pyrolysis of *U. lactuca*, representing 22.63–35.28% of the total relative area. The formation of short-chain carboxylic acids has been linked to the thermal decomposition of lipids. The result of this study is in line with the previous finding of Iaccarino et al. [10], who observed that carboxylic acids were predominantly found in bio-oil from the pyrolysis of Salicornia bigelovii.

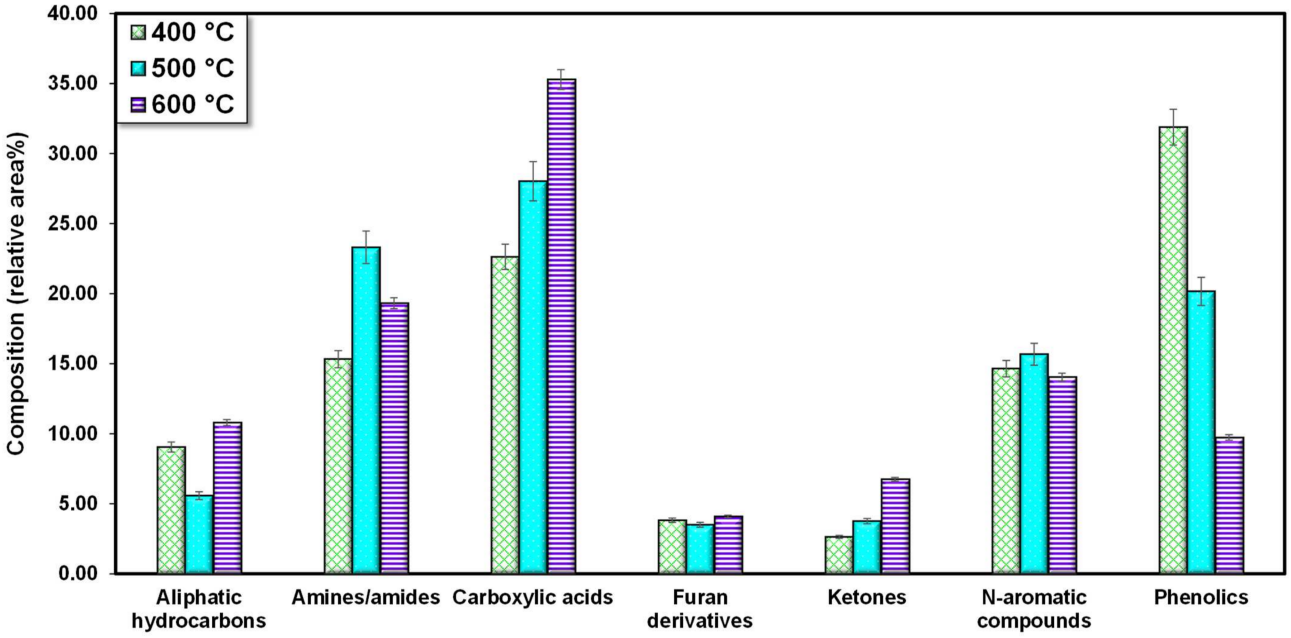

Figure 3. Compounds observed in bio-oil during pyrolysis of *U. lactuca* at 400, 500, and 600 °C.

Phenolic compounds were also observed from the pyrolysis of *U. lactuca*. As previously mentioned, the phenolic compounds might be derived from the steam reaction of aromatic compound. In addition, the formation of phenolic compounds has also been linked to the decomposition of lignin or protein-containing phenylalanine [38]. In this study, it was noticed that the selectivity of phenolic compounds in the bio-oil decreased with an increase in temperature, following the trend: 31.89% (400 °C) > 20.16% (500 °C) > 9.73% (600 °C). This could be attributed to the fact that higher temperatures could promote the cleavage of side chains in phenolic compounds to generate the hydrocarbon [43].

It is worth noting that substantial amine/amide derivatives were observed in the pyrolysis of *U. lactuca*. The relative area of amines/amides was found to be around 15.33, 23.31, and 19.32% at 400, 500, and 600 °C, respectively. The amine/amide derivatives from the pyrolysis of *U. lactuca* were higher than that of other terrestrial lignocellulosic biomass.

Zhang et al. [44] reported that the typical compounds identified from the pyrolysis of lignocellulosic biomass are hydrocarbons, N-containing compounds, alcohols, aldehydes, sugars, phenols, furans, ketones, and acids, and no amine/amide derivatives were observed. This can be explained as being due to the fact that macroalgae have higher protein content than terrestrial lignocellulosic biomass [14]. Amine derivatives are plausibly derived from the decomposition and decarboxylation of amino acids. Meanwhile, the amide compounds might be deduced from the reaction of organic acids and the ammonium produced from the decomposition of amino acids during pyrolysis. The plausible reaction pathways from the slow-pyrolysis of the *U. lactuca* is depicted in Figure 4.

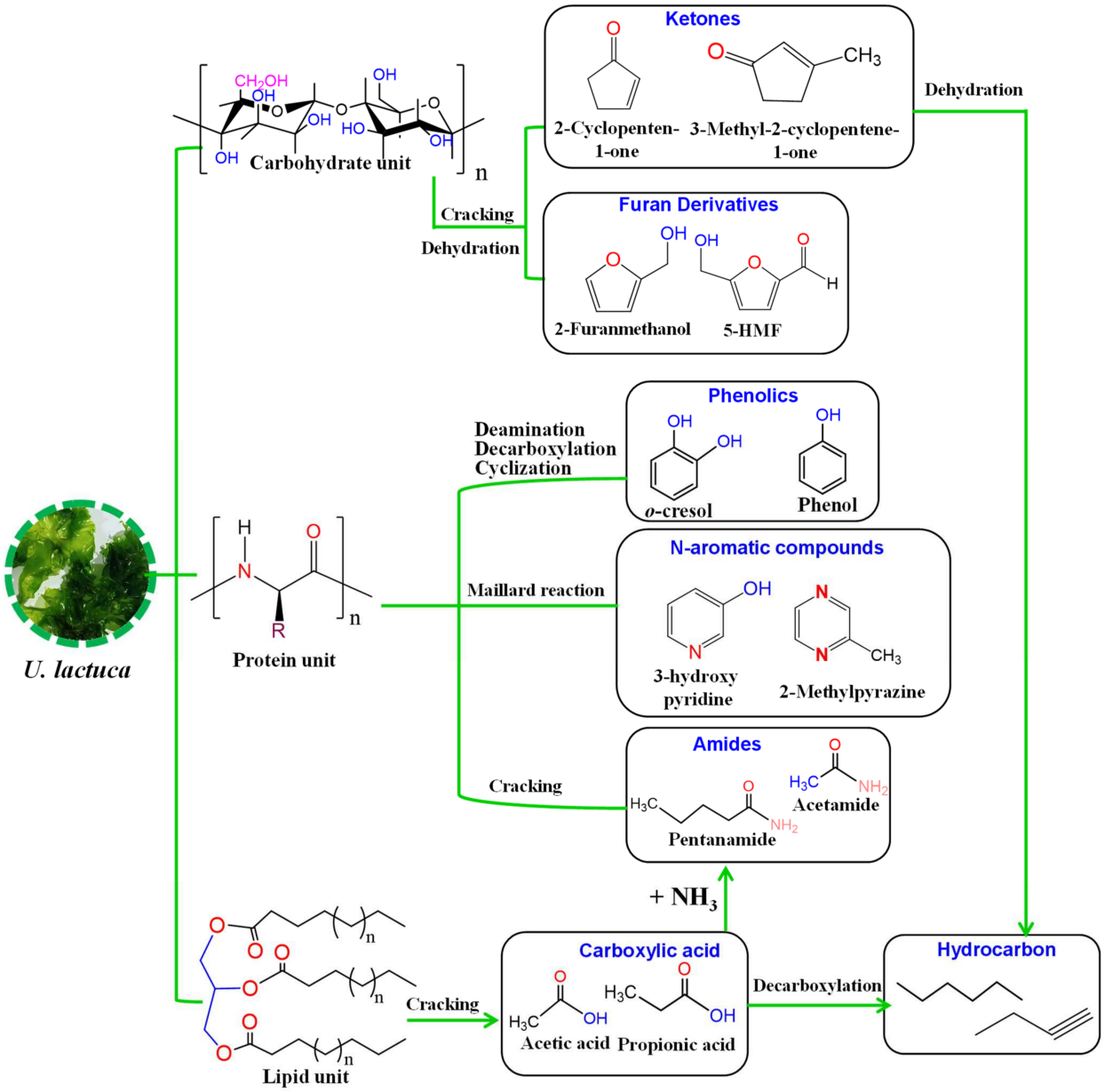

Figure 4. A plausible reaciton pathway of *U. lactuca* decomposition during pyrolysis.

Besides amine/amide derivatives, a significant amount of N-aromatic compounds (14.04–15.68%) were observed in the slow-pyrolysis of *U. lactuca*. The main component of N-aromatic compounds observed in this study was heterocyclic derivatives such as 2-methylpyrazine, 3-methylpyridine, 2-hydroxypyridine, and 5-methylhydantoin. The formation of N-aromatic compounds can be deduced from the deterioration of protein into

amino acids at high pyrolysis temperatures, followed by the cyclization and aromatization reactions of amino acids. Another possibility is the reaction of the amino acids and carbohydrates through the Maillard reaction, which can further decompose to generate N-aromatic compounds [42].

The aliphatic hydrocarbons were also identified in the *U. lactuca*'s bio-oil, which might be generated from the decomposition of long-chain organic acids followed by a decarboxylation reaction. Furthermore, the aliphatic hydrocarbons are plausibly derived from the ring-opening, cracking, and dehydration of cellulose [12]. The small amounts of furan derivatives (i.e., 3.51–4.10%) were observed from the pyrolysis of *U. lactuca*. The typical furan derivatives identified in *U. lactuca*'s bio-oil are 2-furanmethanol, 2-acetylfuran, and 5-methylfurfural (5-HMF). Furan derivatives are generally derived from several steps of dehydration and ring-opening reactions of xylose. Another possibility for furan generation is via a concerted electrocyclic reaction followed by multiple steps of dehydration and cyclization [45]. Finally, trace amounts of ketone derivatives (i.e., 2.64–6.75%) were also identified, which are typical pyrolysis products of cellulose and hemicellulose decomposition [46].

3.3. Biochar Product and Its Characteristics

The ultimate analysis and calorific value of original feedstock and biochar obtained from the pyrolysis of *U. lactuca* at 400, 500, and 600 °C are shown in Table 2. It is clearly shown that the biochar has a higher C content (44.30–48.03%) than the original feedstock (39.1%). The C content in the solid increased with the temperature. However, the O and H contents in the biochar were much lower than those in the original feedstock. The decrease in O and H content could be associated with promoting dehydration and deoxygenation reactions during pyrolysis. The low hydrogen content of biochar has also been linked with the aromatization and formation of hydrogen gas (H_2) as a result of the generation of the low-molecular weight of hydrocarbons [38]. Apart from that, the HHVs of biochar (19.94–21.61 MJ kg^{-1}) obtained from the pyrolysis of *U. lactuca* are much higher than that of the original feedstock (12.04 MJ kg^{-1}). This indicates that the biochar from the pyrolysis of *U. lactuca* can be applied as a solid renewable fuel.

Table 2. Elemental analysis of biochar from pyrolysis of *Ulva lactuca*.

Sample	Ultimate Analysis (wt%, Dry Ash-Free)					HHV (MJ kg^{-1})
	% C	% H	% N	% S	% O	
Ulva lactuca	39.10 ± 0.30	6.20 ± 0.03	4.46 ± 0.02	7.28 ± 0.10	42.96 ± 0.45	12.04 ± 0.06
Biochar (400 °C)	44.30 ± 0.13	4.25 ± 0.17	3.33 ± 0.22	8.41 ± 0.04	39.72 ± 0.47	19.94 ± 0.08
Biochar (500 °C)	45.55 ± 0.06	3.87 ± 0.15	2.91 ± 0.15	9.34 ± 0.08	38.34 ± 0.16	20.50 ± 0.06
Biochar (600 °C)	48.03 ± 0.20	2.39 ± 0.15	2.54 ± 0.18	10.03 ± 0.04	37.01 ± 0.48	21.61 ± 0.09

The Van Krevelen diagram was also presented to investigate the evolution of O/C and H/C atomic ratios during the pyrolysis of *U. lactuca* (Figure 5). The O/C atomic ratio remarkably decreased from 0.82 for *U. lactuca* feedstock to 0.67, 063, and 0.58 for biochar at 400, 500, and 600 °C, respectively. A similar trend with the O/C atomic ratio, the H/C atomic ratio also significantly decreased from 1.90 for *U. lactuca* feedstock to 1.15, 1.02, and 0.60 for biochar at 400, 500, and 600 °C, respectively. The reduction of O/C and H/C atomic ratios of biochar obtained from the pyrolysis of *U. lactuca* could be attributed to the dehydration and decarboxylation reactions that occurred throughout the pyrolysis.

The biochar obtained from the pyrolysis of *U. lactuca* was also characterized by FTIR (Figure 6). Meanwhile, the typical band assignment from the FTIR spectra of biochar obtained from the pyrolysis of *U. lactuca* at different temperatures is summarized in Table S2. The broadband at 3239 cm^{-1} indicated O–H stretching vibration in the biochar at a pyrolysis temperature of 400 °C. However, this peak disappeared when the pyrolysis temperature was increased to 500 and 600 °C, confirming that the dehydration reaction was enhanced with high pyrolysis temperature. The absorption band at 1436 cm^{-1} was assigned in the spectra of biochar, indicating the aliphatic C–H bending. Meanwhile, strong peaks

at 1087 cm^{-1} were observed to stretch vibrations from the C–O group. Moreover, a few peaks at 873 cm^{-1} were observed, indicating the aromatic C–H out-of-plan bending, as Gautam et al. [41] reported. This peak indicated that the biochar contains aromatic compounds. Furthermore, the peaks around 595–873 cm^{-1} have been attributed to the existence of polycyclic aromatic hydrocarbons (PAHs), which could be produced throughout the pyrolysis of biomass [10].

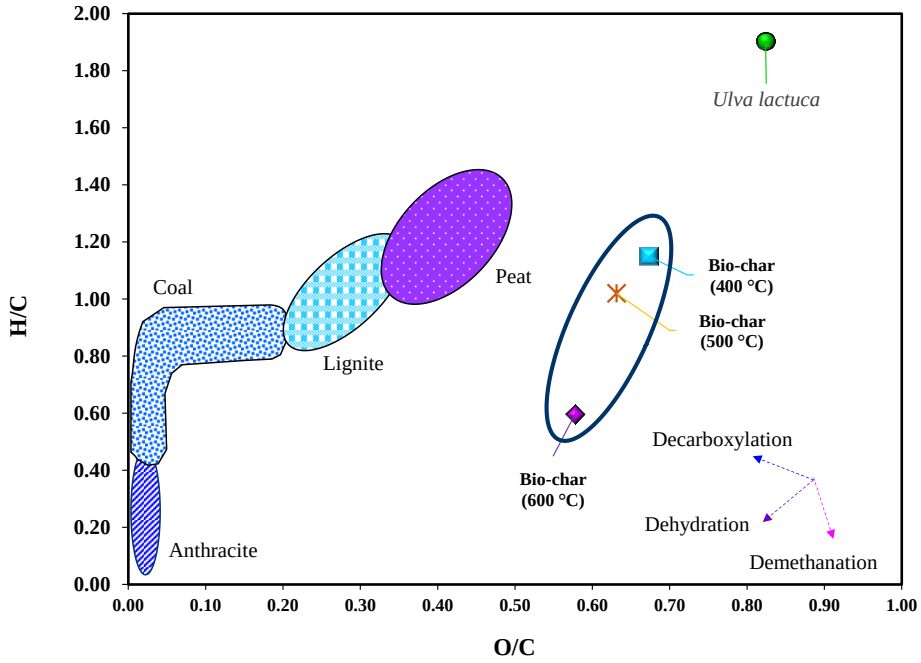

Figure 5. Van Krevelen diagram of the solid product obtained from the pyrolysis of *U. lactuca* at the different reaction temperatures.

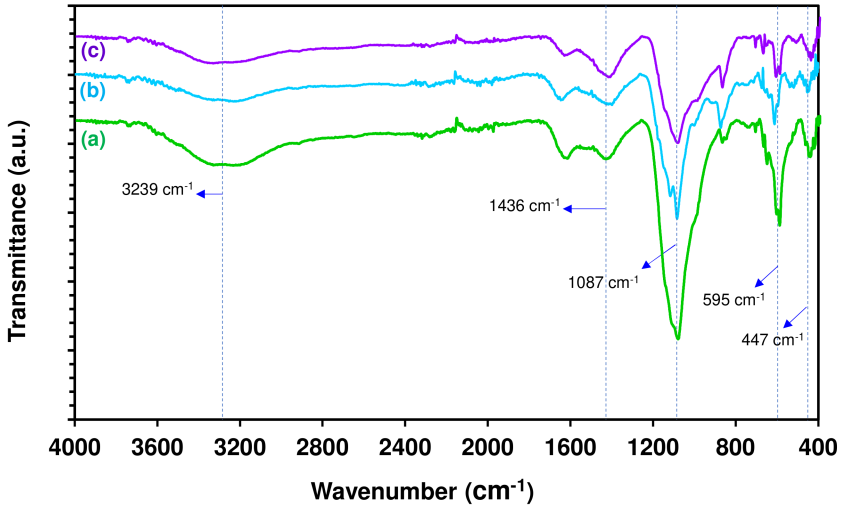

Figure 6. FTIR spectra of biochar obtained from the pyrolysis of *U. lactuca* at (**a**) 400 °C (**b**) 500 °C, and (**c**) 600 °C.

The macroalgal feedstock's surface morphology and its biochar were also observed using SEM (Figure 7). As shown, macroalgal feedstock revealed different properties in terms of morphological structure compared to its solid product. Surprisingly, biochar surface has a higher porosity than the original feedstock. This might be because the high pyrolysis temperature could deform the surface of *U. lactuca*, resulting in the higher porosity structure found in biochar. Furthermore, the pore size of biochar also increased

with the temperature. The pore sizes of the biochar was found to be in the ranges of 4–6 μm, 10–20 μm, and 21–23 μm for pyrolysis temperatures of 400, 500, and 600 °C, respectively. This could be attributed to more organic compounds being decomposed at the higher temperature.

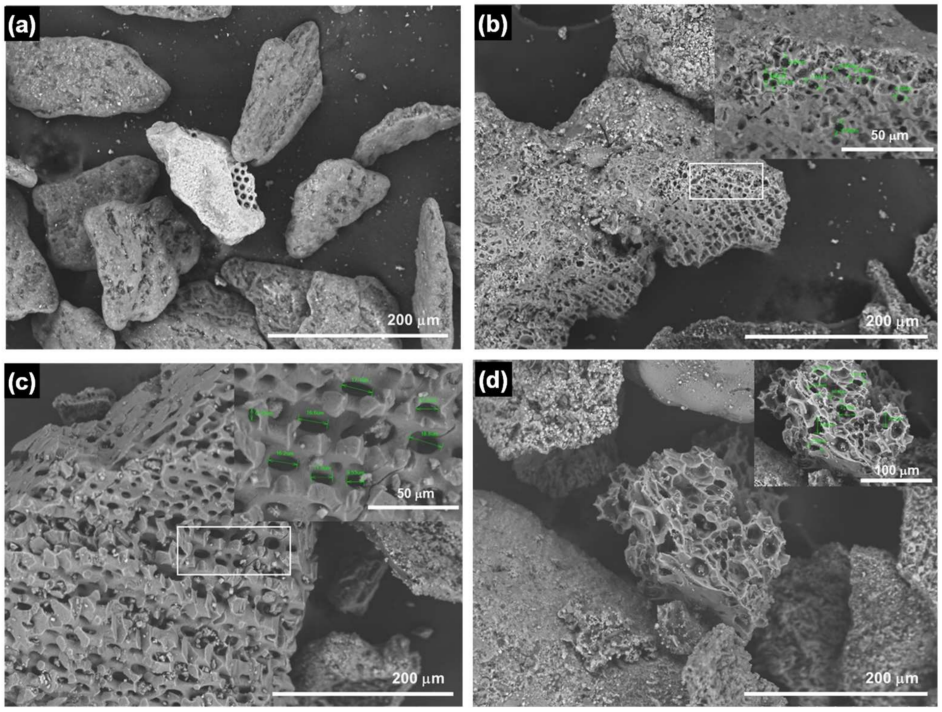

Figure 7. SEM images of (**a**) original feedstock.; (**b**) biochar at 400 °C; (**c**) biochar at 500 °C; and (**d**) biochar at 600 °C.

4. Conclusions

A comprehensive study of the behavior of *U. lactuca* via slow pyrolysis was reported herein to provide a deeper understanding of its valorization. Reaction temperature (400–600 °C) and time (10–50 min) could affect the distribution of bio-oil, biochar, and gas products. An increase in temperature and time increases bio-oil and gas products, but it decreases the biochar yield. This could be due to the significant primary decomposition of macroalgal biomass at higher temperatures or the secondary decomposition of biochar. The maximum bio-oil yield (24.05%) was achieved at 500 °C within 50 min. Meanwhile, the highest biochar yield (88.47%) was obtained at 400 °C within 10 min. The significant compounds obtained in *U. lactuca*'s bio-oil are carboxylic acids (22.63–35.28%), phenolics (9.73–31.89%), amines/amides (15.33–23.31%), and N-aromatic compounds (14.04–15.68%), with the trace amount of aliphatic hydrocarbon, furan derivatives, and ketones. Based on the ultimate analysis, biochar's H/C and O/C atomic ratios were lower than feedstock, confirming that dehydration and decarboxylation reactions occurred throughout the pyrolysis. Higher heating values (HHV) of *U. lactuca*'s biochar (19.94–21.61 MJ kg^{-1}) were much higher than that of the original feedstock (12.04 MJ kg^{-1}), confirming that the biochar from the pyrolysis of *U. lactuca* can be applied as a solid renewable fuel. Intriguingly, SEM analysis exhibited a higher porosity in the biochar surface compared to the original feedstock, indicating that *U. lactuca*'s derived biochar has a great potential as a raw carbon material for synthesizing various functional materials such as catalysts, adsorbents, and energy storage. Overall, the finding highlights that the valorization of *U. lactuca* for environmental mitigation and bioenergy production can be conducted through pyrolysis. Hence, the integrated downstream processes to further valorize *U. lactuca* for bioenergy needs to be conducted in the future.

Supplementary Materials: The following supporting information can be downloaded at https://www.mdpi.com/article/10.3390/su14063233/s1, Figure S1: GC/MS chromatogram from pyrolysis of *U. lactuca* at (a) 400 °C, (b) 500 °C, and (c) 600 °C. Table S1: Proximate and ultimate analysis of *Ulva lactuca*. Table S2: Typical band assignment of biochar from slow pyrolysis of *U. lactuca*.

Author Contributions: Conceptualization, O.F.; Data curation, O.F. and A.B.; Formal analysis, A.A.; Funding acquisition, O.F.; Investigation, A.A. and A.B.; Methodology, A.A. and O.F.; Project administration, O.F.; Resources, A.A., O.F., A.B., N.S. and E.H.; Supervision, E.H. and Y.M.; Writing—original draft, A.A. and O.F.; Writing—review & editing, O.F., A.B., N.S., E.H., N.R.M., S.K. and Y.M. All authors have read and agreed to the published version of the manuscript.

Funding: This research and APC were funded by the Indonesian Endowment Fund for Education (LPDP) and the Indonesian Science Fund (DIPI) through the International Collaboration RISPRO Funding Program "RISPRO KI" (Grant No. RISPRO/KI/B1/KOM/12/11684/1/2020).

Institutional Review Board Statement: Not applicable.

Informed Consent Statement: Not applicable.

Data Availability Statement: Not applicable.

References

1. Destek, M.A.; Sarkodie, S.A.; Asamoah, E.F. Does biomass energy drive environmental sustainability? An SDG perspective for top five biomass consuming countries. *Biomass Bioenergy* **2021**, *149*, 106076. [CrossRef]
2. Biswas, B.; Arun Kumar, A.; Bisht, Y.; Krishna, B.B.; Kumar, J.; Bhaskar, T. Role of temperatures and solvents on hydrothermal liquefaction of Azolla filiculoides. *Energy* **2021**, *217*, 119330. [CrossRef]
3. Leong, Y.K.; Chen, W.-H.; Lee, D.-J.; Chang, J.-S. Supercritical water gasification (SCWG) as a potential tool for the valorization of phycoremediation-derived waste algal biomass for biofuel generation. *J. Hazard. Mater.* **2021**, *418*, 126278. [CrossRef] [PubMed]
4. Ho, S.H.; Zhang, C.; Tao, F.; Zhang, C.; Chen, W.H. Microalgal Torrefaction for Solid Biofuel Production. *Trends Biotechnol.* **2020**, *38*, 1023–1033. [CrossRef]
5. Samanmulya, T.; Farobie, O.; Matsumura, Y. Gasification characteristics of aminobutyric acid and serine as model compounds of proteins under supercritical water conditions. *J. Jpn. Pet. Inst.* **2017**, *60*, 34–40. [CrossRef]
6. Reza, S.; Azad, A.K.; Bakar, M.S.A.; Karim, R.; Sharifpur, M.; Taweekun, J. Evaluation of Thermochemical Characteristics and Pyrolysis of Fish Processing Waste for Renewable Energy Feedstock. *Sustainability* **2022**, *14*, 1203. [CrossRef]
7. Nenciu, F.; Paraschiv, M.; Kuncser, R.; Stan, C.; Cocarta, D.; Vladut, V.N. High-Grade Chemicals and Biofuels Produced from Marginal Lands Using an Integrated Approach of Alcoholic Fermentation and Pyrolysis of Sweet Sorghum Biomass Residues. *Sustainability* **2022**, *14*, 402. [CrossRef]
8. Brindhadevi, K.; Anto, S.; Rene, E.R.; Sekar, M.; Mathimani, T.; Thuy Lan Chi, N.; Pugazhendhi, A. Effect of reaction temperature on the conversion of algal biomass to bio-oil and biochar through pyrolysis and hydrothermal liquefaction. *Fuel* **2021**, *285*, 119106. [CrossRef]
9. Nazir, A.; Laila, U.-; Bareen, F.; Hameed, E.; Shafiq, M. Sustainable Management of Peanut Shell through Biochar and Its Application as Soil Ameliorant. *Sustainability* **2021**, *13*, 13796. [CrossRef]
10. Iaccarino, A.; Gautam, R.; Sarathy, S.M. Bio-oil and biochar production from halophyte biomass: Effects of pre-treatment and temperature on *Salicornia bigelovii* pyrolysis. *Sustain. Energy Fuels* **2021**, *5*, 2234–2248. [CrossRef]
11. Casoni, A.I.; Ramos, F.D.; Estrada, V.; Diaz, M.S. Sustainable and economic analysis of marine macroalgae based chemicals production—Process design and optimization. *J. Clean. Prod.* **2020**, *276*, 122792. [CrossRef]
12. Adams, J.M.M.; Toop, T.A.; Donnison, I.S.; Gallagher, J.A. Seasonal variation in Laminaria digitata and its impact on biochemical conversion routes to biofuels. *Bioresour. Technol.* **2011**, *102*, 9976–9984. [CrossRef] [PubMed]
13. Milledge, J.J.; Smith, B.; Dyer, P.W.; Harvey, P. Macroalgae-derived biofuel: A review of methods of energy extraction from seaweed biomass. *Energies* **2014**, *7*, 7194–7222. [CrossRef]

14. Farobie, O.; Matsumura, Y.; Syaftika, N.; Amrullah, A.; Hartulistiyoso, E.; Bayu, A.; Moheimani, N.R.; Karnjanakom, S.; Saefurahman, G. Recent advancement on hydrogen production from macroalgae via supercritical water gasification. *Bioresour. Technol. Rep.* **2021**, *16*, 100844. [CrossRef]
15. Liu, J.; Tong, Y.; Xia, J.; Sun, Y.; Zhao, X.; Sun, J.; Zhao, S.; Zhuang, M.; Zhang, J.; He, P. *Ulva* macroalgae within local aquaculture ponds along the estuary of Dagu River, Jiaozhou Bay, Qingdao. *Mar. Pollut. Bull.* **2022**, *174*, 113243. [CrossRef]
16. Bews, E.; Booher, L.; Polizzi, T.; Long, C.; Kim, J.H.; Edwards, M.S. Effects of salinity and nutrients on metabolism and growth of *Ulva lactuca*: Implications for bioremediation of coastal watersheds. *Mar. Pollut. Bull.* **2021**, *166*, 112199. [CrossRef]
17. Gao, G.; Clare, A.S.; Rose, C.; Caldwell, G.S. *Ulva rigida* in the future ocean: Potential for carbon capture, bioremediation and biomethane production. *GCB Bioenergy* **2018**, *10*, 39–51. [CrossRef]
18. Cheney, D.; Rajic, L.; Sly, E.; Meric, D.; Sheahan, T. Uptake of PCBs contained in marine sediments by the green macroalga *Ulva rigida*. *Mar. Pollut. Bull.* **2014**, *88*, 207–214. [CrossRef]
19. Nielsen, M.M.; Bruhn, A.; Rasmussen, M.B.; Olesen, B.; Larsen, M.M.; Møller, H.B. Cultivation of *Ulva lactuca* with manure for simultaneous bioremediation and biomass production. *J. Appl. Phycol.* **2012**, *24*, 449–458. [CrossRef]
20. Rinehart, S.; Guidone, M.; Ziegler, A.; Schollmeier, T.; Thornber, C. Overwintering strategies of bloom-forming *Ulva* species in Narragansett Bay, Rhode Island, USA. *Bot. Mar.* **2014**, *57*, 337–341. [CrossRef]
21. Human, L.R.D.; Adams, J.B.; Allanson, B.R. Insights into the cause of an *Ulva lactuca Linnaeus* bloom in the Knysna Estuary. *S. Afr. J. Bot.* **2016**, *107*, 55–62. [CrossRef]
22. Milledge, J.J.; Harvey, P.J. Golden Tides: Problem or golden opportunity? The valorisation of *Sargassum* from beach inundations. *J. Mar. Sci. Eng.* **2016**, *4*, 60. [CrossRef]
23. Kang, E.J.; Han, A.R.; Kim, J.H.; Kim, I.N.; Lee, S.; Min, J.O.; Nam, B.R.; Choi, Y.J.; Edwards, M.S.; Diaz-Pulido, G.; et al. Evaluating bloom potential of the green-tide forming alga *Ulva ohnoi* under ocean acidification and warming. *Sci. Total Environ.* **2021**, *769*, 144443. [CrossRef] [PubMed]
24. Qi, L.; Hu, C. To what extent can *Ulva* and *Sargassum* be detected and separated in satellite imagery? *Harmful Algae* **2021**, *103*, 102001. [CrossRef]
25. Salimi, P.; Norouzi, O.; Pourhoseini, S.E.M.; Bartocci, P.; Tavasoli, A.; Di Maria, F.; Pirbazari, S.M.; Bidini, G.; Fantozzi, F. Magnetic biochar obtained through catalytic pyrolysis of macroalgae: A promising anode material for Li-ion batteries. *Renew. Energy* **2019**, *140*, 704–714. [CrossRef]
26. Ly, H.V.; Choi, J.H.; Woo, H.C.; Kim, S.S.; Kim, J. Upgrading bio-oil by catalytic fast pyrolysis of acid-washed *Saccharina japonica* alga in a fluidized-bed reactor. *Renew. Energy* **2019**, *133*, 11–22. [CrossRef]
27. Hao, J.; Qi, B.; Li, D.; Zeng, F. Catalytic co-pyrolysis of rice straw and ulva prolifera macroalgae: Effects of process parameter on bio-oil up-gradation. *Renew. Energy* **2021**, *164*, 460–471. [CrossRef]
28. Brigljević, B.; Liu, J.J.; Lim, H. Comprehensive feasibility assessment of a poly-generation process integrating fast pyrolysis of *S. japonica* and the Rankine cycle. *Appl. Energy* **2019**, *254*, 113704. [CrossRef]
29. Kostas, E.T.; Williams, O.S.A.; Duran-Jimenez, G.; Tapper, A.J.; Cooper, M.; Meehan, R.; Robinson, J.P. Microwave pyrolysis of *Laminaria digitata* to produce unique seaweed-derived bio-oils. *Biomass Bioenergy* **2019**, *125*, 41–49. [CrossRef]
30. Alves, J.L.F.; Da Silva, J.C.G.; da Silva Filho, V.F.; Alves, R.F.; Ahmad, M.S.; Ahmad, M.S.; de Galdino, W.V.A.; De Sena, R.F. Bioenergy potential of red macroalgae *Gelidium floridanum* by pyrolysis: Evaluation of kinetic triplet and thermodynamics parameters. *Bioresour. Technol.* **2019**, *291*, 121892. [CrossRef]
31. Wu, P.; Zhang, X.; Wang, J.; Yang, J.; Xuanwei, P.; Feng, L.; Zu, B.; Xie, Y.; Li, M. Pyrolysis of aquatic fern and macroalgae biomass into bio-oil: Comparison and optimization of operational parameters using response surface methodology. *J. Energy Inst.* **2021**, *97*, 194–202. [CrossRef]
32. Verma, T.N.; Shrivastava, P.; Rajak, U.; Dwivedi, G.; Jain, S.; Zare, A.; Shukla, A.K.; Verma, P. A comprehensive review of the influence of physicochemical properties of biodiesel on combustion characteristics, engine performance and emissions. *J. Traffic Transp. Eng.* **2021**, *8*, 510–533. [CrossRef]
33. Ma, C.; Geng, J.; Zhang, D.; Ning, X. Non-catalytic and catalytic pyrolysis of *Ulva prolifera* macroalgae for production of quality bio-oil. *J. Energy Inst.* **2020**, *93*, 303–311. [CrossRef]
34. Ceylan, S.; Goldfarb, J.L. Green tide to green fuels: TG-FTIR analysis and kinetic study of *Ulva prolifera* pyrolysis. *Energy Convers. Manag.* **2015**, *101*, 263–270. [CrossRef]
35. Liu, W.J.; Jiang, H.; Yu, H.Q. Development of Biochar-Based Functional Materials: Toward a Sustainable Platform Carbon Material. *Chem. Rev.* **2015**, *115*, 12251–12285. [CrossRef] [PubMed]
36. Amrullah, A.; Farobie, O.; Pramono, G.P. Solid degradation and its kinetics on phenol-rich bio-oil production from pyrolysis of coconut shell and Lamtoro wood residue. *Korean J. Chem. Eng.* **2022**, *39*, 389–397. [CrossRef]
37. Amrullah, A.; Farobie, O.; Widyanto, R. Pyrolysis of purun tikus (*Eleocharis dulcis*): Product distributions and reaction kinetics. *Bioresour. Technol. Rep.* **2021**, *13*, 100642. [CrossRef]
38. Aboulkas, A.; Hammani, H.; El Achaby, M.; Bilal, E.; Barakat, A.; El Harfi, K. Valorization of algal waste via pyrolysis in a fixed-bed reactor: Production and characterization of bio-oil and bio-char. *Bioresour. Technol.* **2017**, *243*, 400–408. [CrossRef]
39. Yan, L.; Wang, Y.; Li, J.; Zhang, Y.; Ma, L.; Fu, F.; Chen, B.; Liu, H. Hydrothermal liquefaction of *Ulva prolifera* macroalgae and the influence of base catalysts on products. *Bioresour. Technol.* **2019**, *292*, 121286. [CrossRef]

40. Choi, J.H.; Kim, S.S.; Suh, D.J.; Jang, E.J.; Min, K., II; Woo, H.C. Characterization of the bio-oil and bio-char produced by fixed bed pyrolysis of the brown alga *Saccharina japonica*. *Korean J. Chem. Eng.* **2016**, *33*, 2691–2698. [CrossRef]
41. Gautam, R.; Shyam, S.; Reddy, B.R.; Govindaraju, K.; Vinu, R. Microwave-assisted pyrolysis and analytical fast pyrolysis of macroalgae: Product analysis and effect of heating mechanism. *Sustain. Energy Fuels* **2019**, *3*, 3009–3020. [CrossRef]
42. Wang, S.; Xia, Z.; Wang, Q.; He, Z.; Li, H. Mechanism research on the pyrolysis of seaweed polysaccharides by Py-GC/MS and subsequent density functional theory studies. *J. Anal. Appl. Pyrolysis* **2017**, *126*, 118–131. [CrossRef]
43. Kim, J.Y.; Moon, J.; Lee, J.H.; Jin, X.; Choi, J.W. Conversion of phenol intermediates into aromatic hydrocarbons over various zeolites during lignin pyrolysis. *Fuel* **2020**, *279*, 118484. [CrossRef]
44. Zhang, L.; Yang, Z.; Li, S.; Wang, X.; Lin, R. Comparative study on the two-step pyrolysis of different lignocellulosic biomass: Effects of components. *J. Anal. Appl. Pyrolysis* **2020**, *152*, 104966. [CrossRef]
45. Zhou, X.; Li, W.; Mabon, R.; Broadbelt, L.J. A mechanistic model of fast pyrolysis of hemicellulose. *Energy Environ. Sci.* **2018**, *11*, 1240–1260. [CrossRef]
46. Reyes, L.; Abdelouahed, L.; Mohabeer, C.; Buvat, J.C.; Taouk, B. Energetic and exergetic study of the pyrolysis of lignocellulosic biomasses, cellulose, hemicellulose and lignin. *Energy Convers. Manag.* **2021**, *244*, 114459. [CrossRef]